Received: 31 July 2020 | Revised: 27 October 2020 | Accepted: 14 December 2020

DOI: 10.1111/nan.12682

Neuropathology and Applied Neurobiology WILEY

ORIGINAL ARTICLE

Effects of mutant huntingtin inactivation on Huntington disease-related behaviours in the BACHD mouse model

Rachel Y. Cheong[1] | Barbara Baldo[1] | Muhammad U. Sajjad[1] | Deniz Kirik[2] | Åsa Petersén[1]

[1]Translational Neuroendocrine Research Unit, Department of Experimental Medical Science, Lund University, Lund, Sweden

[2]Brain Repair and Imaging in Neural Systems Unit, Department of Experimental Medical Science, Lund University, Lund, Sweden

Correspondence
Rachel Y. Cheong, Translational Neuroendocrine Research Unit, Department of Experimental Medical Science, Lund University, BMC D11, 221 84 Lund, Sweden.
Email: rachel.cheong@med.lu.se

Present address
Barbara Baldo, Evotec SE, HD Research and Translational Sciences, Hamburg, Germany

Funding information
This work was supported in parts by grants from the Swedish Research Council to DK and ÅP (K2012-99X-22330-01-5, 2013/03537 and 2018/02559), the Province of Skåne State Grants (ALF) to ÅP and grants from the Royal Physiographic Society of Lund (2015-36140), Lars Hiertas Foundation (FO2015-0100) and NEURO Sweden to RYC. ÅP is a Wallenberg Clinical Scholar (Knut and Alice Wallenberg Foundation, #2019.0467). The funding bodies had no role in the design of the study, collection, analysis and interpretation of data or in writing the manuscript.

Abstract

Aims: Huntington disease (HD) is a fatal neurodegenerative disorder with no disease-modifying treatments approved so far. Ongoing clinical trials are attempting to reduce huntingtin (HTT) expression in the central nervous system (CNS) using different strategies. Yet, the distribution and timing of HTT-lowering therapies required for a beneficial clinical effect is less clear. Here, we investigated whether HD-related behaviours could be prevented by inactivating mutant HTT at different disease stages and to varying degrees in an experimental model.

Methods: We generated mutant BACHD mice with either a widespread or circuit-specific inactivation of mutant HTT by using Cre recombinase (Cre) under the nestin promoter or the adenosine A_{2A} receptor promoter respectively. We also simulated a clinical gene therapy scenario with allele-specific HTT targeting by injections of recombinant adeno-associated viral (rAAV) vectors expressing Cre into the striatum of adult BACHD mice. All mice were assessed using behavioural tests to investigate motor, metabolic and psychiatric outcome measures at 4–6 months of age.

Results: While motor deficits, body weight changes, anxiety and depressive-like behaviours are present in BACHD mice, early widespread CNS inactivation during development significantly improves rotarod performance, body weight changes and depressive-like behaviour. However, conditional circuit-wide mutant HTT deletion from the indirect striatal pathway during development and focal striatal-specific deletion in adulthood failed to rescue any of the HD-related behaviours.

Conclusions: Our results indicate that widespread targeting and the timing of interventions aimed at reducing mutant HTT are important factors to consider when developing disease-modifying therapies for HD.

KEYWORDS
Adenosine A_{2A} receptor, striatum, Huntington disease, BACHD, indirect striatal pathway

Abbreviations: BSA, bovine serum albumin ; CNS, central nervous system; Cre, Cre recombinase; DAB, diaminobenzidine tetrahydrochloride; DARPP-32, dopamine- and cAMP-regulated phosphoprotein of relative molecular mass 32; DEXA, dual energy x-ray absorptiometry; EPM, elevated plus maze; EYFP, enhanced yellow fluorescent protein; FST, forced swim test; GABA, Gamma-amino-butyric acid; GFAP, glial fibrillary acidic protein; GFP, green fluorescent protein; HD, Huntington disease; HTT, huntingtin; OF, open field; PBS, phosphate buffer saline; PDE10A, cAMP and cAMP-inhibited cGMP 3', 5'-cyclic phosphodiesterase 10A; polyQ, polyglutamine; PVDF, polyvinylidene fluoride; rAAV, recombinant adeno-associated virus; rpm, revolutions per minute; TBS, tris-buffered saline; TBS-T, tris-buffered saline with tween-20; WT, wild-type.

Deniz Kirik and Åsa Petersén have contributed equally

INTRODUCTION

Although both mutant and wild-type forms of huntingtin (HTT) are ubiquitously expressed in Huntington's disease (HD), certain neuronal circuitries in the central nervous system (CNS) are selectively affected. In particular, the striatum is the most affected region in HD and pathology in this area is thought to be involved in the development of motor disturbances. Dopamine D2 receptor-expressing neurons of the indirect pathway are thought to be among the first neurons to be affected in HD [1-5]. Despite the lack of any approved disease-modifying treatments for HD at present, there are a number of ongoing and planned clinical trials attempting to reduce HTT expression in the CNS using different strategies [6-8]. Within the field, there is currently extensive discussion regarding the distribution and timing of HTT-lowering therapies. This has implications for both therapeutic development and understanding fundamental biological processes in HD. From a therapeutic perspective, there are questions regarding what extent of the CNS and which specific circuitries need to be targeted to yield a beneficial clinical effect. The therapeutic window to intervene for a clinically meaningful effect to occur is not known. In light of an increasing number of publications indicating a critical effect of mutant HTT in development [9-12], it is possible that the expression of mutant HTT during development has already induced key toxic effects to such an extent that inactivation of mutant HTT after that phase renders little or no effect once the disease process has started. These aspects have converged as important questions to address so as to advance the development of disease-modifying therapies.

In order to address these pressing questions, we have designed the following genetic experiments using the well-established BACHD mouse model. This model has been engineered to express full-length mutant HTT and manifests a phenotype with motor, psychiatric and metabolic disturbances [13-15]. As mutant HTT is 'floxed', cross-breeding with other mice expressing Cre recombinase enables the generation of mutant lines without expression of mutant HTT in selected cell populations and/or brain regions [16-21]. We first aimed to remove mutant HTT early during development in a widespread fashion within the CNS by crossing BACHD mice with Nestin-Cre mice, with the hypothesis that these animals would show significant improvements. The aim was to investigate whether their phenotype would completely normalise given that peripheral pathology has also been suggested to play a role in HD [22-26]. We then refined the design and limited the inactivation of mutant HTT selectively to dopamine D2 receptor-expressing projection neurons of the indirect striatal pathway. In order to circumvent the main caveat of using a dopamine D2 receptor-Cre mouse which would have resulted in recombination not only in the indirect pathway of the striatum but also in the substantia nigra pars compacta, we used adenosine A_{2A} receptor-Cre mice. Adenosine A_{2A} and dopamine D2 receptors are co-expressed on D2 receptor-expressing neurons in the indirect pathway [27-29]. Finally, we wanted to simulate a clinical scenario with focal administration of gene therapy with allele-specific targeting to the striatum, the most affected region in HD. We used intra-striatal injections of a clinically applicable rAAV vector to mediate gene transfer of Cre. This approach would target a large area of the striatum without distinguishing between different subpopulations of striatal neurons.

MATERIALS AND METHODS

The complete experimental procedure can be found in Appendix A: Supplementary Material and Methods.

Animals

All mice were housed in cages of 4–6 animals under conditions of 12-hour light/dark cycles (lights on at 07:00 h) with *ad libitum* access to normal chow and water. All procedures were approved by the Lund University Animal Welfare and Ethics committee under permit M65-13 and M124-15.

Experiment I: CNS-specific HTT deletion from the entire brain during development

Mutant lines were generated by Cre-LoxP transgenesis using 'floxed' C57BL6/J BACHD mice and Nestin-Cre driver mice. The resultant offspring consisted of mutant mice (BACHD-Nestin or BACHD) and wild-type littermate controls (Nestin-Cre and WT). Mice were subjected to behavioural tests between 4–6 months of age.

Experiment II: HTT deletion from the indirect striatal pathway during development

Mutant lines were generated by Cre-LoxP transgenesis using 'floxed' BACHD mice on the C57BL6/J background and the adenosine A_{2A}-Cre driver mice. Mating was designed to generate mutant mice (BACHD-A_{2A} or BACHD) alongside wild-type littermate controls (A_{2A}-Cre and WT). Mice were subjected to behavioural tests at 6 months of age. To visualise Cre expression in A_{2A}-expressing cells, the A_{2A}-Cre driver line was crossed with the ROSA-EYFP reporter mouse line.

Experiment III: rAAV-vector-mediated HTT deletion from the striatum at adult stage

Adult BACHD and WT mice on the FVB/N background were bilaterally injected with a recombinant adeno-associated viral (rAAV) vector expressing the Cre recombinase enzyme under the control of a

synthetic CBA promoter (rAAV5-CBA-Cre) or with formulation buffer solution matching the ones used for viral suspension. Behavioural tests were performed 3 months after surgery at the age of 5 months. To verify the efficiency of recombination, ROSA-EYFP reporter mice were also injected with the rAAV-CBA-Cre vector and processed for GFP immunohistochemistry.

Validation of Cre recombination excision

To detect mutant *HTT* alleles recombined by Cre, genomic DNA was extracted from dissected tissue from the striatum, cerebral cortex, hypothalamus and cerebellum using standard DNA isolation methods. Recombination by Cre generates a band around 600 bp and an unrecombined allele results in a band around 1050 bp.

AAV vector production and surgery

The viral vector used in this study was produced as previously described [15]. About 0.75 µl of the vector was deposited at a speed of 0.20 µl per minute over 4 minutes at four injection sites to cover the striatum: 1.4 mm and 0.9 mm posterior to bregma, 1.7 mm and 2.1 mm medial and lateral to bregma and 3.0 mm ventral to the dura (total 1.5 µl/hemisphere).

Behavioural tests

All mice underwent a battery of behavioural tests for total locomotor activity, motor coordination, gait, anxiety-like and depressive-like behaviours at 4–6 months of age. All behavioural tests were performed during the light phase of the light/dark cycle and handled by the same group of experimenters.

Immunohistochemistry

Mice were transcardially perfused first with 4% paraformaldehyde, brains were cryoprotected in a 25% sucrose solution and cut. Six series of 30-µm thick coronal sections were collected and processed for immunohistochemistry.

Single label GFP and Cre immunohistochemistry

Sections were treated with 3% hydrogen peroxide and 10% methanol to quench endogenous peroxidase activity and pre-incubated in 5% normal goat serum prior to incubation in chicken polyclonal primary antisera directed against GFP (1:100,000; #AB13970; Abcam; Cambridge, UK) or rabbit polyclonal antisera directed against Cre recombinase (1:30,000; #PRB-106C; Covance, Princeton, NJ, USA) in Tris buffered saline (TBS) containing 1% bovine serum albumin (BSA) and 0.25% Triton X-100 overnight at room temperature. Sections were then incubated in their respective biotinylated secondary immunoglobulins (1:200; Vector Laboratories Inc, Burlingame, CA, USA) for 1 hour at room temperature. After subsequent washing in TBS, the sections were incubated in Vectastain Elite avidin-peroxidase kit (1:50; Vector Laboratories) for 1 hour at room temperature. Peroxidase labelling was visualised with diaminobenzidine tetrahydrochloride (DAB) using 1% hydrogen peroxidase which resulted in a brown precipitate. The estimated volume of Cre coverage in the striatum was measured using the Computer Assisted Toolbox Software (New CAST) module in the Visiopharm VIS software (Version 4.5.5.433, Visiopharm A/S, Horsholm, Denmark).

Double label GFAP + Cre and NeuN + Cre immunohistochemistry

Double label peroxidase free-floating immunohistochemistry was undertaken to verify the percentage of neurons and astrocytes targeted with the rAAV-CBA-Cre vector. In brief, sections were first incubated in rabbit polyclonal antisera directed against Cre recombinase. Immunoreactivity was revealed with nickel-enhanced DAB using 1% hydrogen peroxidase which resulted in a black precipitate within the nucleus of the labelled cell. Sections were further incubated in rabbit polyclonal antisera against glial fibrillary acidic protein (GFAP; 1:500; #Z0034, DAKO) or in mouse monoclonal antisera against neuronal nuclei (NeuN; 1:500, #MAB377, Millipore) using the same protocol described above for single label immunohistochemistry and processed using DAB only as a chromogen. The percentage of GFAP- and NeuN-positive cells expressing Cre recombinase was determined with unbiased stereology using the Visiopharm VIS software.

Western blot

For analysis of mutant HTT protein levels, fresh frozen striatal samples were collected for Western blot. Protein lysates were loaded on a 3–8% gradient gel (Tris-acetate Precast Gel, Bio-Rad) before being transferred onto a polyvinylidene fluoride (PVDF) membrane using the Bio-Rad Trans-Blot Turbo Transfer System. Membranes were blotted with rabbit monoclonal primary antisera directed against HTT (1:1000, #AB109115, Abcam), rabbit monoclonal primary antisera directed against PDE10A (1:10,000, #AB227829, Abcam), rabbit polyclonal primary antisera directed against DARPP-32 (1:1000, #TA309102, Origene) or mouse monoclonal primary antisera directed against beta-actin (1: 10,000, #A1978, Sigma-Aldrich). Membranes were then probed with their respective secondary antibodies, developed and analysed with densitometry.

Statistical analysis

All data are presented as group means ±SEM. Statistical analyses were conducted using the SPSS statistical software (SPSS Version 25, IBM Inc., Chicago, IL, USA). Normality of the residuals distribution was first verified using linear regression. In cases where the data did not follow a normal Gaussian distribution, the entire data were transformed into the log10 or square root scale and the residuals of the transformed data were plotted again to ensure a normal distribution. The data were then analysed using a two-way ANOVA followed by a post-hoc unpaired Student's t-test when appropriate to determine differences between genotype (presence of HTT) and treatment (presence of Cre). Statistical significance was accepted at $p < 0.05$. A full report of the statistical results is presented in the Appendix B: Supplementary Statistical Results.

RESULTS

Widespread HTT deletion in the CNS during early development results in reduced HTT levels and substantial reversal of HD-related behaviours

In order to achieve an early and widespread inactivation of mutant HTT selectively in the CNS, we crossed Nestin-Cre with BACHD mice to generate offspring with the conditional deletion of mutant HTT exon 1 from Nestin-expressing cells by Cre recombinase (Figure 1A). We verified the efficiency of Cre excision in BACHD-Nestin mice. The unrecombined intact *HTT* exon 1 allele (1050 bp) was detected in BACHD brain and liver samples while the recombined excised *HTT* exon 1 allele (600 bp) was strongly detected only in BACHD-Nestin brain samples (Figure 1B), indicative of recombination in a CNS-specific manner. Western blot analyses revealed HTT protein levels remaining in the striatum to determine the degree of HTT reduction. The expected HTT band of ~350 kDa was detected in BACHD and BACHD-Nestin samples with the upper mutant HTT band absent from WT, Nestin-Cre and BACHD-Nestin samples (Figure 1C). Further densitometry analyses indicated a 57% loss of HTT in BACHD-Nestin mice compared to BACHD mice ($p < 0.0001$, Figure 1C). This agrees with our previous study showing a similar reduction of mutant HTT in these mice, measured with an AlphaLISA assay [30]. In addition, we also assessed levels of two highly enriched proteins in the striatum that are affected by the *HTT* gene, cAMP and cAMP-inhibited cGMP 3',5'-cyclic phosphodiesterase 10A (PDE10A) and dopamine- and cAMP-regulated phosphoprotein of relative molecular mass 32 (DARPP-32). While striatal levels of PDE10A and DARPP-32 appear to be lower in BACHD compared to WT mice, no statistically significant differences were detected between the genotypes (two-way ANOVA for PDE10A; genotype $p = 0.265$; two-way ANOVA for DARPP-32; genotype $p = 0.085$; n = 8/genotype, Appendix C, Supplementary Figure 1A,B). Hence in this cohort of mice, the trend towards a reduction of these protein levels in BACHD mice at 4–6 months of age is not sufficiently large

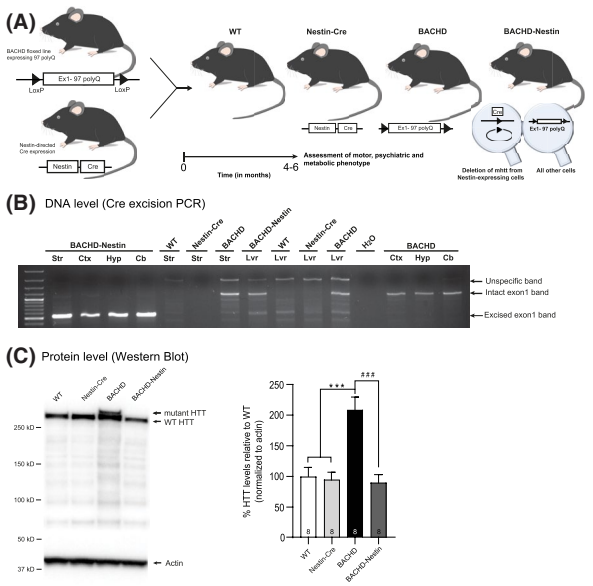

FIGURE 1 Validation of widespread HTT deletion from the entire brain during development. (A) Generation of the BACHD-Nestin mutant mouse line by crossing male BACHD mice with female mice expressing Cre recombinase under the Nestin promoter (Nestin-Cre). The resultant offspring comprises of WT mice expressing endogenous mouse HTT (WT), Nestin-Cre mice, BACHD mice, and mice in which mutant HTT has been selectively deleted from A_{2A}-expressing cells (BACHD-A_{2A}). (B) Gel showing PCR products detected in several brain regions and liver samples from BACHD-Nestin, WT, Nestin-Cre and BACHD mice. The presence of the unmodified mutant HTT allele (1050 bp; arrow labelled intact exon 1) was detected in all brain regions from BACHD samples as well as in all liver samples from both BACHD and BACHD-Nestin samples. The recombined mutant HTT allele (600 bp; arrow labelled excised exon 1) was detected only in the brain samples from BACHD-Nestin mice. (C) Representative Western blot image showing mutant and WT HTT protein levels from the striatum of WT, Nestin-Cre, BACHD and BACHD-Nestin mice using the AB109115 antibody, Abcam. The mutant HTT band was absent in striatal samples from WT, Nestin-Cre and BACHD-Nestin mice. Quantification of Western blots with densitometry analysis indicates a significant reduction of HTT protein levels in BACHD-Nestin samples. Data presented as mean ±SEM, ***$p < 0.001$ represents a genotype difference, ### $p < 0.001$ represents an effect of mutant HTT deletion, two-way ANOVA. The number of animals used in each group is indicated in the bars.

to allow detection of a potential effect of a HTT-lowering strategy. This is also in agreement with previous studies that reported no significant differences in the levels of DARPP-32 protein in the striatum of 10-month old BACHD mice [31] or in PDE10A binding using the selective tracer ^{3}H-7980 between BACHD and WT mice at 8, 10 and 12 months of age [32].

To determine whether mutant HTT deletion restricted to the CNS is sufficient to revert motor dysfunction, we performed a series of behavioural tests to assess motor function. The first task was on the accelerating rotarod which evaluates motor coordination and balance. By the end of the training phase, all mice, regardless of sex

and genotype, reached a stable baseline performance (Figure 2A,C). For the accelerating rotarod task, mice were placed on a rotating beam which underwent a linear acceleration from 4 to 40 rpm over 5 minutes. Both female and male BACHD mice had a reduced latency to fall, indicative of deficits in coordination and balance ($p < 0.05$ in females and $p < 0.001$ in males, Figure 2B,D). Interestingly, a CNS-specific mutant HTT deletion completely improves the rotarod performance in females but not in males ($p < 0.05$, Figure 2B). We assessed other parameters of motor function with the open field test to evaluate general locomotor activity and the footprints test

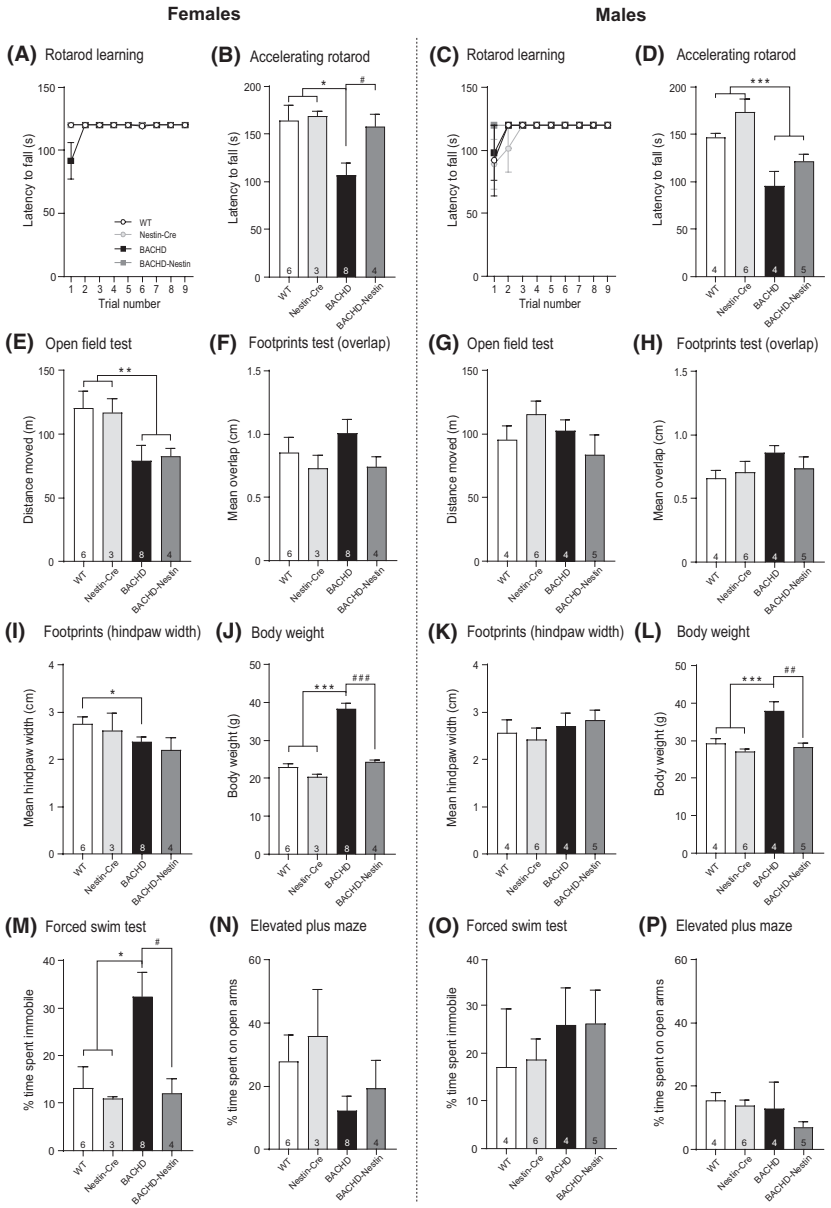

FIGURE 2 CNS-specific HTT deletion results in substantial reversal of HD-related behaviours. (A-D) Rotarod learning during the training phase; both female (A) and male (C) BACHD and BACHD-Nestin mice attained a baseline performance after 3 days of training. Motor coordination and balance was assessed with the accelerating rotarod task. Bar graphs show latency to fall off the rotarod. Both female (B) and male (D) BACHD-Nestin mice show significant improvements in motor coordination and balance. (E, G) General locomotor activity was measured using the open field test. Female BACHD and BACHD-Nestin mice show reduced activity over 1 hour. (F, H, I, K) Bar graphs show mean overlap between the forepaw and hindpaw in the footprint test and the width between the left and right hindpaw. (J, L) Body weight measurements indicate a complete reversal of the metabolic phenotype in BACHD-Nestin mice. (M, O) The forced swim test (FST) was used as a measure of behavioural despair. Bar graphs show percentage of time spent being immobile. Female BACHD-Nestin mice show significant improvements of depressive-like behaviour with reductions in the time spent immobile compared to BACHD mice. (N, P) The elevated plus maze (EPM) was used as a measure of anxiety-like behaviour. The more anxious the animal, the less time spent on the open arms of the EPM. Data presented as mean ±SEM, ***$p < 0.001$, *$p < 0.05$ represents a genotype difference, ### $p < 0.001$, ## $p < 0.01$, # $p < 0.05$ represents an effect of mutant HTT deletion, two-way ANOVA. The exact number of animals used in each group is indicated in the bars.

to evaluate gait abnormalities. Only BACHD females but not males displayed altered function compared to WT mice but there was no effect of the CNS-specific mutant HTT deletion (Figure 2E-I,K). The pronounced metabolic phenotype in BACHD mice of both sexes was completely rescued with the deletion of mutant HTT from the CNS ($p < 0.001$, Figure 2J,L). Next, we assessed the effects of a CNS-wide mutant HTT deletion on the psychiatric phenotype in BACHD mice. Depressive-like behaviours, analysed with the forced swim test as a measure of behavioural despair, were only detected in female BACHD mice and these behaviours were completely abolished with the deletion of mutant HTT from the CNS ($p < 0.05$, Figure 2M,O). Anxiety-like behaviours were absent in this cohort of BACHD mice at 4–6 months of age (Figure 2N,P).

HTT deletion from the indirect striatal pathway does not improve motor, metabolic or psychiatric disturbances

Next, we wanted to test the effects of mutant HTT inactivation on the earliest affected striatal neurons in HD, the D2 receptor-expressing neurons of the indirect striatal pathway. We generated mice with the conditional elimination of mutant HTT exon 1 from adenosine A_{2A} receptor-expressing cells from birth (Figure 3A). This adenosine A_{2A}-Cre line has been shown to induce specific recombination only in the indirect striatal pathway [33,34]. We first verified the targeting of A_{2A} receptor-expressing cells in A_{2A}-Cre;ROSA-EYFP mice with GFP immunohistochemistry. GFP immunohistochemistry revealed a heterogeneous distribution of cells exhibiting both neuronal and glial-like profiles in the striatum and to a lesser extent in the cortex, hypothalamus and cerebellum (Figure 3B). This is in line with previous studies showing a high distribution of A_{2A} receptors in the dorsal and ventral striatum but also in extra-striatal regions such as the cerebellum and hypothalamus [35]. PCR analysis on dissected brain regions indicated that the recombined excised *HTT* exon 1 allele was only detected in BACHD-A_{2A} samples (Figure 3C). The recombined band was detected in the striatum, hypothalamus, cortex and cerebellum of BACHD-A_{2A} mice suggesting that recombination occurs in these regions, which is in line with the results generated from A_{2A}-Cre;ROSA-EYFP reporter mice. Quantification of remaining HTT protein levels with densitometry revealed a 21% reduction of mutant HTT in the BACHD-A_{2A} mice compared to BACHD mice ($p < 0.05$, Figure 3D).

To determine if mutant HTT deletion from the adenosine A_{2A} cell population would be sufficient for rescuing HD motor, metabolic and psychiatric dysfunction, we similarly performed a series of behavioural tests. For the accelerating rotarod task, both female and male BACHD and BACHD-A_{2A} mice had a reduced latency to fall, indicating that they had difficulties coordinating and balancing on the beam and fell off significantly faster than their WT counterparts ($p < 0.05$, Figure 4A-D). Despite this, there was no difference between BACHD and BACHD-A_{2A} (Figure 4A-D). Similar to the accelerating rotarod, there were no improvements in motor dysfunction with the open field and footprints tests in BACHD-A_{2A} mice of both sexes (Figure 4E-H). No differences were detected in the stride length and hindpaw width (data not shown). Taken together, the motor phenotype in BACHD mice is not ameliorated by inactivating mutant HTT in D2 receptor-expressing neurons of the indirect striatal pathway.

Dopamine D2 receptor-expressing neurons in the striatum have been suggested to be involved in the regulation of appetite and body weight control [36,37]. BACHD and BACHD-A_{2A} mice, regardless of sex, weighed significantly heavier than their WT counterparts ($p < 0.0001$, Figure 4I,K). However, the deletion of mutant HTT from A_{2A} receptor-expressing cells did not alter body weight (Figure 4I,K). These changes in body weight corresponded to the percentage body fat ($p < 0.0001$, Figure 4J,L) with no effect of mutant HTT deletion from A_{2A} receptor-expressing cells (Figure 4J,L). Lastly, we sought to determine if there was any rescue of the psychiatric phenotype. Both female and male BACHD and BACHD-A_{2A} mice spent significantly more time being immobile in the FST compared to control mice, indicative that there was no improvement of the depressive-like behaviour with the absence of mutant HTT from A_{2A} receptor-expressing cells (Figure 4M,O). Similarly, female BACHD mice displayed anxiety-like behaviours with this behaviour observed to a similar extent in BACHD-A_{2A} mice (Figure 4N). Male mice in this cohort did not exhibit any anxiety-like behaviours at 6 months of age (Figure 4P). Hence, the inactivation of mutant HTT in D2 receptor-expressing neurons of the indirect striatal pathway does not ameliorate the metabolic or psychiatric phenotype in this model.

rAAV vector-mediated HTT deletion from the striatum at the adult stage results in reduced HTT levels but no rescue of HD-related behaviours

Finally, we wanted to simulate a clinical scenario with rAAV vector-mediated inactivation of mutant HTT in the striatum of adult BACHD mice. To achieve this, bilateral striatal stereotaxic injections were performed on BACHD mice with rAAV-CBA-Cre at 2 months of age to ablate mutant HTT from the striatum (Figure 5A). Immunohistochemical analysis for Cre expression together with volume measurement showed vector coverage of about 75% of the striatum with a denser core of vector deposit constituting about 50% of the striatum (Figure 5B-C,E). There was also transduction of cortical cells especially in the deeper layers of the cortex where about 10% of cortex was labelled (Figure 5D,F). To verify the transduction efficiency, the rAAV-CBA-Cre vector was injected into ROSA-EYFP reporter mice and processed for GFP+Cre immunohistochemistry. Cre-positive cells co-localised with GFP-positive cells, exhibiting neuronal and glial-like profiles in the striatum and to a much lesser extent in the cortex (Figure 5G). In order to validate the type of cells targeted, rAAV-CBA-Cre-injected mice were stained for GFAP+Cre (Figure 5H) and NeuN+Cre (Figure 5I). Stereological analysis revealed that 57.0 ± 2.0% of GFAP-positive astrocytes and 47.6 ± 1.9% of NeuN-positive neurons were co-localised with Cre. In addition,

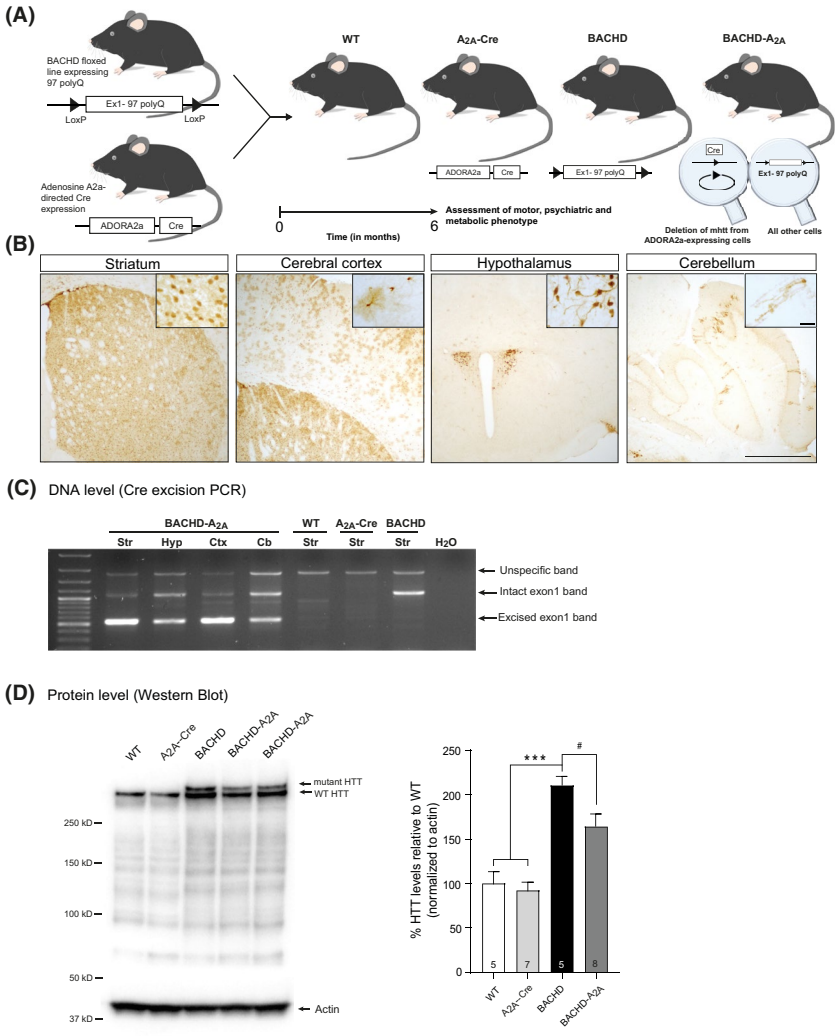

FIGURE 3 HTT deletion from the dopamine D2 receptor-expressing neurons in the indirect striatal pathway using adenosine A_{2A}-cre mice. (A) Schematic representation depicting the generation of the BACHD-A_{2A} mutant mouse line by crossing male BACHD mice with female mice expressing Cre recombinase under the adenosine A_{2A} promoter. (B) Representative photomicrographs of GFP immunoreactivity, indicative of recombination, in the striatum, cortex, hypothalamus and cerebellum of a BACHD-A_{2A} mouse crossed with the ROSA-EYFP reporter mouse. Scale bar corresponds to 100 µm and insert 20 µm. (C) Gel showing PCR products detected in several brain regions from BACHD-A_{2A}, WT, A_{2A}-Cre and BACHD mice. The presence of the unmodified mutant HTT allele was detected in all brain regions in the BACHD-A_{2A} and BACHD samples. The recombined mutant HTT allele was only detected in the striatum, cortex, hypothalamus and cerebellum from BACHD-A_{2A} mice. (D) Representative Western blot image showing the reduction in mutant HTT protein levels in BACHD-A_{2A} mice using the AB109115 antibody, Abcam. WT and A_{2A}-Cre mice show absence of the WT HTT band. The beta-actin blot serves as loading control. Quantification of Western blots with densitometry analysis indicates a significant reduction of HTT protein levels in BACHD-A_{2A} mice. Data presented as mean ±SEM, ***$p < 0.001$ represents a genotype difference, # $p < 0.05$ represents an effect of mutant HTT deletion, two-way ANOVA. The exact number of animals used in each group is indicated in the bars.

the proportion of neurons to astrocytes detected was ~92.0 ± 2.9% and 8.0 ± 2.9% respectively (data not shown). On the genomic DNA level, we confirmed excision by Cre in dissected brain regions from buffer- or Cre-injected WT and BACHD mice (Figure 5J). While not quantitative, the recombined band appeared stronger in the striatum of Cre-injected BACHD mice compared to the cortex from the same animal. We measured HTT protein levels with Western Blot where the upper mutant band was detected only in BACHD buffer and Cre-injected samples, while the lower wild-type band was present in all groups (Figure 5K). Densitometry analyses revealed a 40% reduction in protein levels between BACHD buffer and Cre samples ($p < 0.05$, Figure 5K).

Motor behaviour was assessed with the accelerating rotarod, open field and footprints test. Although deficits in motor coordination were detected in female BACHD mice with the accelerating rotarod task, deletion of mutant HTT from the striatum was not sufficient to rescue motor coordination (Figure 6A,B). Similarly, general locomotor activity was significantly and equally affected in female BACHD buffer- and Cre-injected mice with the open field test ($p < 0.001$, Figure 6C). Using the

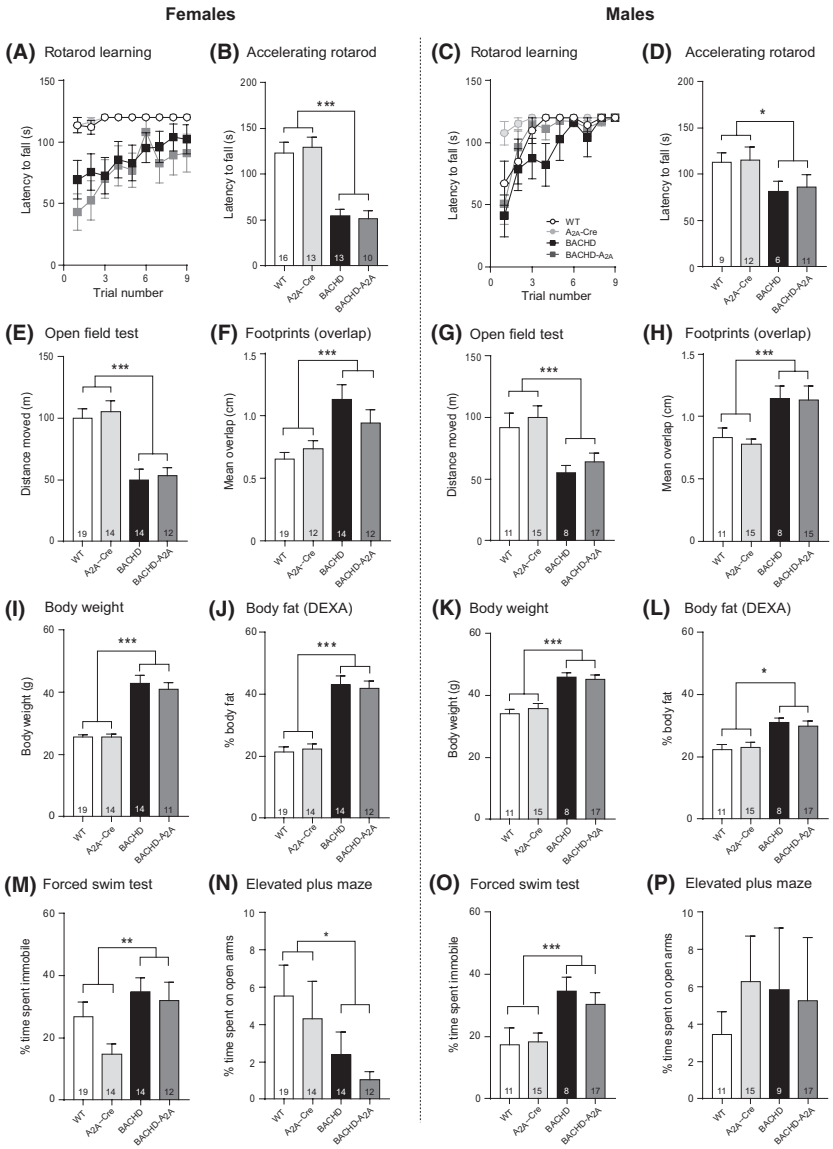

FIGURE 4 Motor, psychiatric and metabolic phenotype after mutant HTT ablation from the A_{2A} receptor-expressing neurons in the indirect striatal pathway. (A, C) Line graphs show rotarod learning during the training phase. Female (A) and male (C) BACHD and BACHD-A_{2A} mice eventually attained a baseline performance after 3 days. (B, D) Motor coordination and balance were assessed with the accelerating rotarod. Bar graphs show latency to fall on the accelerating rotarod. BACHD and BACHD-A_{2A} mice have decreased latency to fall, implicating impairment with motor coordination and balance. (E, G) General locomotor activity was measured using the open field test. BACHD and BACHD-A_{2A} mice show reduced activity over 1 hour. (F, H) Bar graphs show mean overlap between the forepaw and hindpaw in the footprint test, indicative of abnormalities in gait. Both male and female BACHD and BACHD-A_{2A} mice show increased mean overlap compared to their WT littermates. (I-L) Bar graphs show body weight measurements at 6 months of age in females (I) and in males (K). BACHD and BACHD-A_{2A} mice have significantly elevated body weight compared to WT and A_{2A}-Cre controls. Whole body dual energy x-ray absorptiometry (DEXA) measurements show a corresponding increase in body fat at 6 months of age in females (J) and males (L, M, O) BACHD and BACHD-A_{2A} mice, regardless of sex, exhibit depressive-like behaviours which are not improved with the conditional deletion of mutant HTT from the indirect striatal pathway. (N, P) Female BACHD and BACHD-A_{2A} mice (N) spent less time exploring the open arms of the EPM while there was no difference detected in male mice (P). Data presented as mean ±SEM, ***$p < 0.001$, *$p < 0.05$, two-way ANOVA. The exact number of animals used in each group is indicated in the bars.

footprints test, we found an effect of genotype in which female BACHD mice had increased measured mean hindpaw width and overlap compared to WT mice ($p < 0.01$, Figure 6D,E), indicative of motor disturbances in female BACHD mice. Interestingly, we found an amelioration of motor dysfunction in Cre-injected BACHD mice assessed with the mean hindpaw width compared to BACHD buffer-injected mice ($p < 0.001$, Figure 6E). There was no effect of Cre injection on the mean stride length (data not shown) and overlap between the fore- and hindpaw (Figure 6D). No significant differences were detected in males for any of the behavioural tests assessing motor function (Appendix C, Supplementary Figure S2A-C).

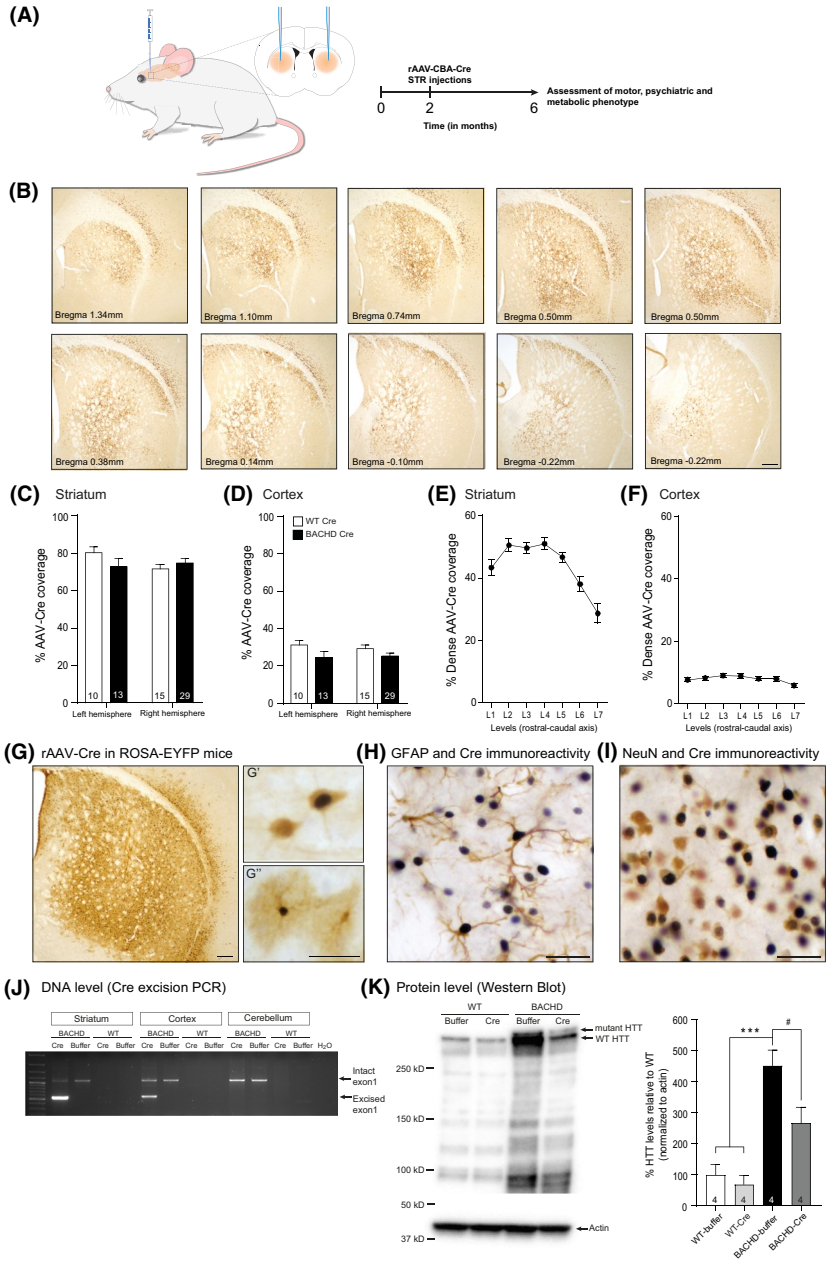

FIGURE 5 Validation of AAV-vector-mediated deletion of mutant HTT from the striatum in adult BACHD mice. (A) Schematic diagram of the experiment. (B) Photomicrographs showing Cre immunoreactivity and the extent of viral vector spread in the striatum and in the deep layers of the cortex. (C D) Estimation of Cre coverage in the striatum and cortex. Bar graph shows Cre coverage of the viral vector in the striatum (C) and cortex (D) of bilaterally injected WT and BACHD mice. e, f. Estimated Cre coverage from the dense core in the striatum and cortex. Line graph shows Cre coverage in seven consecutive sections (180 µm apart, L1 to L7 in the rostral to caudal axis) in the striatum (E) and cortex (F, G) Verification of transduction efficiency. Dual-label immunohistochemical photomicrographs from Cre-injected ROSA-EYFP reporter mice showing GFP (brown) and Cre (black) immunoreactivity. High-powered magnification showing a dual-labelled cell with a neuronal-like profile (G') and a dual-labelled cell with glial-like profile (G''). Scale bar represents 100 µm (G) and 20 µm (G' and G''). (H, I) Representative photomicrographs showing dual-labelling of GFAP-positive astrocytes (brown) expressing Cre (black) (H) as well as dual-labelled NeuN-positive neurons (brown) expressing Cre (black) (I) in the striatum. Scale bar represents 20 µm. (J) Gel showing PCR products from Cre- or buffer-injected WT and BACHD mice. The recombined mutant HTT allele (600 bp; arrow labelled excised exon 1) was detected only in the striatum and to a lesser extent the cortex of BACHD Cre-injected mice. (K) Bar graph shows the amount of mutant HTT relative to beta-actin levels in BACHD buffer and Cre-injected mice after densitometry quantification of Western blots using the HTT AB109115 antibody. Data presented as mean ±SEM, two-way ANOVA, ***$p < 0.0001$ effect of genotype, # $p < 0.05$ effect of treatment. The exact number of animals used in each group is indicated in the bars.

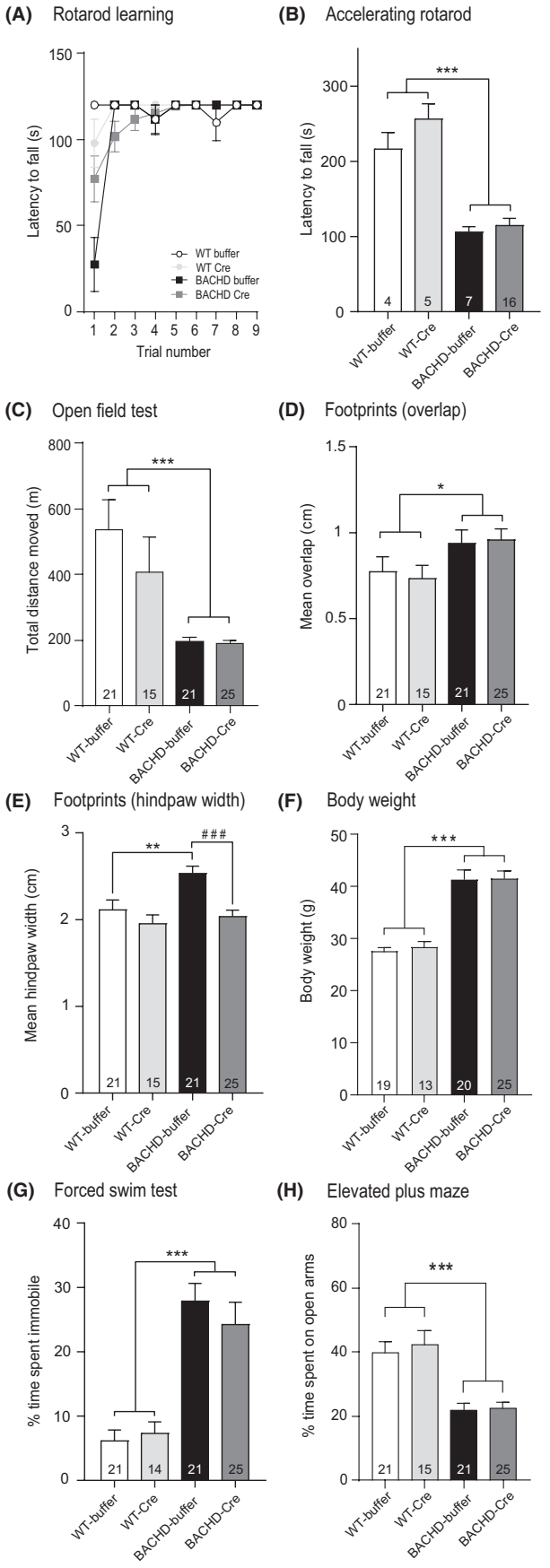

FIGURE 6 Effects on HD-related behaviours in female BACHD mice after AAV-vector-mediated mutant HTT inactivation. (A) Rotarod learning during the training phase. All mice eventually attained a baseline performance after 3 days of training. (B) Motor coordination was assessed with the accelerating rotarod task. Bar graphs show latency to fall off the rotarod. Female BACHD buffer- and Cre-injected mice exhibit significant deficits in motor coordination and balance on the accelerating rotarod. (C) General locomotor activity as assessed with the open field test. BACHD mice, regardless of treatment, show deficits with motor activity. (D-E) Analyses of gait with the footprints test with bar graphs showing the mean overlap and mean hindpaw width. BACHD Cre-injected mice show improvements in the hindpaw width assessment of the footprints test. (F) Body weight measurements at 6 months of age. Both buffer- and Cre-injected BACHD mice have increased body weight compared to controls. (G) The forced swim test (FST) was used as a measure of behavioural despair. BACHD mice show increased percentage of time spent immobile, regardless of treatment. (H) Bar graph shows the percentage of time spent on the open arms of the elevated plus maze. Data presented as mean ±SEM, ***$p < 0.0001$, **$p < 0.001$, *$p < 0.05$, represents a genotype difference, ### $p < 0.0001$, represents an effect of Cre-mediated mutant HTT deletion, two-way ANOVA. The exact number of animals used in each group is indicated in the bars.

Body weight was assessed every four weeks from the day of surgery (data not shown). We found that deletion of mutant HTT in the striatum did not lead to significant changes in body weight (Figure 6F). Similarly, the deletion of mutant HTT with Cre recombinase did not affect body weight in males (Appendix C, Supplementary Figure S2D). In terms of depressive-like behaviours, we found that both BACHD buffer- and Cre-injected female mice spent significantly more time immobile compared to their WT counterparts ($p < 0.001$, Figure 6G). Despite this, depressive-like behaviours in BACHD mice remain unaltered after deletion of mutant HTT in the striatum (Figure 6G). This was similar in males (Appendix C, Supplementary Figure S2E). In terms of anxiety-like behaviours, female BACHD mice on the FVB/N background spend significantly less percentage time on the open arms compared to WT mice regardless of treatment on the elevated plus maze ($p < 0.001$, Figure 6H) but deletion of mutant HTT from the striatum did not improve anxiety-like behaviours (Figure 6H). Male BACHD mice on the FVB/N strain at 6 months of age in this study failed to exhibit typical anxiety-like behaviours (Appendix C, Supplementary Figure S2F).

DISCUSSION

This is an era of intense therapeutic development aimed at lowering HTT levels using a variety of molecular tools and delivery methods. During this time, it has become clear that fundamental questions remain unanswered regarding what brain regions need to be targeted

and at what stage of the disease process in order to generate a disease-modifying and meaningful clinical effect. Our results indicate that widespread CNS inactivation of mutant HTT during development significantly improves rotarod performance, body weight changes and depressive-like behaviour. In contrast, conditional mutant HTT inactivation in the indirect striatal pathway during development with the adenosine A_{2A} genetic crossing and region-specific mutant HTT deletion in the striatum during adulthood with viral vectors failed to rescue any of the HD-related behavioural phenotype. Together, these data highlight the importance of distribution and timing of mutant HTT inactivation for beneficial outcome measures.

Motor dysfunction is a key component of HD and is required for a clinical diagnosis according to international guidelines [38]. In agreement with a substantial number of studies using the BACHD model, we demonstrate deficits in coordination and balance with the accelerating rotarod, deficits in locomotor activity with the open field test and gait abnormalities in the footprints test with both strains of BACHD mice at 6 months of age [13,31,39,40]. Implicit to the approaches used in this study is the underlying assumption that motor function is controlled by the striatum, in particular the dopamine D2 receptor-expressing neurons of the striatum. We used the adenosine A_{2A} receptor-Cre mice to indirectly assess the effects of inactivating mutant HTT from the indirect striatal pathway. Studies have shown that adenosine A_{2A} receptors can influence the function and survival of striatal neurons and altering its activity may have an impact on the pathophysiology of HD [41-44]. However, we did not find any rescue of motor dysfunction with the cell type selective mutant HTT deletion from cells expressing adenosine A_{2A} receptors in BACHD mice. A recent study by Burrus and colleagues reported that wild-type HTT in the indirect striatal pathway is important for motor function, as conditional HTT deletion from the indirect striatal pathway with similar adenosine A_{2A}-Cre mice leads to hyperactivity in mice [34]. Similarly, conditional HTT deletion in the direct striatal pathway led to hypoactivity and reduced motor coordination, indicating that loss of WT HTT in the striatum may play a key role in the development of motor symptoms in HD [34].

Furthermore, the rAAV-vector-mediated mutant HTT inactivation approach from the striatum did not result in any reversal of the general locomotor behaviour and motor coordination, despite our results showing a clear rescue of motor deficits in the hindpaw width suggesting a reversal in gait abnormalities as observed in female Cre-injected BACHD mice. As this is the only positive observation from the different motor tests conducted, this might be seen as evidence for residual plasticity in the striatal neurons. Intriguingly, it appears that a 21% and 40% reduction in overall mutant HTT protein levels detected in the striatum of BACHD-A_{2A} and Cre-injected mice respectively proved futile in preventing the development of HD-related behaviours in BACHD mice. Based on this finding, it seems likely that a higher proportion of mutant HTT reduction in the striatum is warranted in order to obtain overall beneficial effects on behaviour. Correction of these behavioural abnormalities might require a more complete deletion of mutant HTT expression in the striatum and/or coverage of other affected cells or tissue. It would be interesting to determine the proportion of indirect versus direct striatal pathway targeted from the rAAV-vector-mediated mutant HTT inactivation approach as both these pathways may be required for a functional control of movement. The lack of any overt reversal of motor behaviour with the A_{2A}-Cre and rAAV-vector-mediated approaches suggests the importance of other non-cell type-specific effects of mutant HTT. Alternatively, although surprising, it is possible that there may be other parallel motor networks in play which are perhaps more critical for the motor abnormalities in BACHD mice. In support of this, a case has been made for the combinatory interacting role between mutant HTT in the striatum and cortex with beneficial effects on the motor phenotype when mutant HTT was deleted concomitantly in the striatum and cortex as compared to the partial amelioration with deletion in the striatum alone [16,45]. A future challenge for the field would be to develop methodologies that allow for multiple parallel pathways to be modulated simultaneously. It is also likely that the targeting of key cell populations for producing effects on motor function is dependent on disease stage. Recent studies have suggested that there may already be important changes early during development in HD and that mutant HTT may impair striatal development in HD mice [9-11,46,47]. Interestingly, inactivation of mutant HTT throughout the CNS and the periphery at 3 weeks of age in BACHD mice using a tamoxifen-inducible approach failed to prevent the development of motor impairments and striatal neurodegeneration later in adult life [12]. This suggests that the window for therapeutic intervention to prevent the development of HD-related impairments in adulthood is likely to be very early on, even before the onset of any detectable early symptoms [48].

Nestin is considered to be a marker for neural stem/progenitor cells and is expressed during development in most cells of the CNS [49]. As Nestin is expressed on embryonic day 7.5 when the brain starts to form in mice [50], inactivation of mutant HTT at this early stage is likely to be sufficient for preventing the potential developmental effects of mutant HTT within the CNS. A previous study found that mutant HTT deletion from all cells with CNS origin significantly improved rotarod performance, striatal volume and body weight [20]. In that same study, cultured primary microglia from BACHD-Nestin mice showed a similar interleukin-6 secretion profile to microglia isolated from BACHD mice after controlled standard endotoxin stimulation, indicative that microglia are unaffected in BACHD-Nestin mice [20]. While we also found significant improvements in motor coordination, assessed by rotarod performance, it is intriguing that other aspects of motor behaviour such as gait and total locomotor activity were not fully reversed in BACHD-Nestin mice. Activated microglia are present in post-mortem striatal tissue from HD brains [51] and have been suggested to play a role in causing striatal neuropathology and motor disturbances through effects induced by mutant HTT in these cells [52-56]. Although a previous study showed that mutant HTT deletion in microglia alone was not sufficient to ameliorate motor disturbances in BACHD mice [20], it is possible that both microglia and cells with CNS origin need to be targeted to fully prevent the

development of a HD-like phenotype. Furthermore, Nestin is expressed in peripheral tissues with muscle and endothelial origins such as skeletal muscle and kidney [57], and it is therefore possible that prevention of pathology in these peripheral tissues could contribute to the motor phenotype rescue in the BACHD-Nestin mice. It should also be noted that peripheral pathology has been detected in other non-Nestin-expressing tissues such as the heart, liver and white adipose tissue in HD and it remains possible that pathology in these areas contributes to the non-rescued motor dysfunction in BACHD-Nestin mice [22-26].

Non-motor symptoms such as psychiatric and metabolic disturbances are common across the HD disease spectrum [58]. D2 receptor-expressing neurons in the striatum have been suggested to play a role in obesity as well as in psychiatric disturbances [37,59-61]. Although we did not find any effect of cell-specific and region-specific mutant HTT inactivation on the development of psychiatric and metabolic changes, the complete rescue of these behaviours in the BACHD-Nestin crossing indicates a CNS origin. The hypothalamus is a key regulator of emotion, metabolism and sleep, and this brain region has been implicated in the non-motor features of HD [62,63]. In clinical HD, hypothalamic changes have indeed been shown to occur prior to motor dysfunction using magnetic resonance imaging and positron emission tomography [64,65], suggesting that the hypothalamus might be affected early in the HD pathological process. Neuropathological studies have also shown that emotion- and metabolism-regulating neuronal populations are affected in the HD hypothalamus [63,66-71]. Importantly, our previous work in experimental models of HD, including the BACHD mouse, has established a causative link between the expression of mutant HTT in the hypothalamus and the development of metabolic dysfunction [15]. In fact, we have shown that deletion of mutant HTT in the hypothalamus in BACHD mice ameliorates both depressive-like behaviours and metabolic disturbances suggesting that hypothalamic dysfunction may be important for the non-motor phenotype in this model [14,15]. Our study further supports this notion of non-motor HD behaviours having a CNS-specific origin whereby depressive and metabolic behaviours in BACHD mice were completely reversed with a CNS-specific deletion of mutant HTT from Nestin-expressing cells.

While the BACHD mouse model recapitulates several of the HD-related features, all animal models ultimately have their intrinsic caveats whereby they will not fully mimic the entire disease progression. As such, caution must always be taken when interpreting and extrapolating results generated from animal models. The BACHD mouse differs from clinical HD in several important ways (reviewed in [72]). One important difference is the genetic construct with two endogenous mouse *Htt* genes besides the human mutant *HTT* gene which affects outcomes where levels of WT and mutant HTT are important. It is also constructed with a mixed CAG/CAA repeat containing 51% CAA (49 CAA out of 97 CAG/CAA) and hence significantly differs also in this regard to the human mutant *HTT* gene [31]. This may be important as somatic instability depends on the length of uninterrupted CAG repeats and influences disease progression in HD [73,74]. Also, HD toxicity may be induced by CAG repeats in the RNA transcript that lead to secondary structures affecting alternative splicing mechanisms, which are modified by CAA interruptions [75-77]. Furthermore, besides the expression of a polyglutamine-expanded protein in HD, both sense and antisense repeat-associated non-ATG (RAN) proteins have been shown to be present in the striatum in human post-mortem tissue from HD patients [78] It has been suggested that the mixed CAG/CAA repeat form a complex hairpin-containing structure that may produce additional novel di-peptide RAN proteins, which may contribute to the phenotype in BACHD mice [78]. However, whether RAN proteins are indeed expressed and contribute to the phenotype in BACHD mice need to be studied.

With the ultimate goal of developing a therapy capable of reducing mutant HTT expression, there has been an increase in the development of various strategies targeting the DNA with zinc-finger proteins and antisense oligonucleotides or siRNAs targeting the RNA [7,79-84]. Given the importance of wild-type HTT during development and for maintaining synaptic function, the earliest time-point for treatment and the long-term effects of lowering or reducing both wild-type and mutant HTT non-selectively are not known. The future challenge for HD therapeutics would be to develop allele-specific therapies to target multiple circuitries in parallel at the earliest possible time-point so as to prevent and/or delay the onset of the disease.

CONCLUSIONS

Our findings show that a CNS-wide early inactivation of mutant HTT reverses aspects of HD-related behaviours, whilst both cell type-specific early inactivation of mutant HTT from the indirect striatal pathway and region-specific inactivation from the striatum alone in adulthood failed to show any behavioural improvements. The circuits controlling motor behaviours are complex and likely to require simultaneous targeting of other brain regions and/or neurocircuits. These new observations highlight the importance of the timing and extent of mutant HTT inactivation on the HD behavioural outcome which may impact upon the future development of disease-modifying therapies for HD.

ACKNOWLEDGEMENTS

We thank Björn Anzelius, Anneli Josefsson, Anna Hansen, Ulla Samuelsson and Ulrika Sparrhult-Björk at Lund University for their valuable technical assistance. We also thank Drs. Sofia Hult Lundh, Rana Soylu-Kucharz and Gabrielle Callander for their initial contributions in evaluating potential striatal coordinates for stereotaxic surgeries. BACHD mice were provided by Dr. X. William Yang at Semel Institute and David Geffen School of Medicine at UCLA.

CONFLICT OF INTERESTS

The authors declare that they have no competing interests.

AUTHOR'S CONTRIBUTION

RYC, DK and ÅP conceived and designed experiments. RYC and BB performed experiments and analysed the data. MUS performed experiments. RYC, DK and ÅP wrote the manuscript. All authors read and approved the final manuscript.

ETHICS APPROVAL AND CONSENT TO PARTICIPATE

All procedures were approved by the Lund University Animal Welfare and Ethics committee under permit M65-13 and M124-15.

CONSENT FOR PUBLICATION

Not applicable.

PEER REVIEW

The peer review history for this article is available at https://publons.com/publon/10.1111/nan.12682.

DATA AVAILABILITY STATEMENT

The datasets analysed in this study are available from the corresponding author on reasonable request.

ORCID

Rachel Y. Cheong https://orcid.org/0000-0003-0264-7636
Åsa Petersén https://orcid.org/0000-0001-5488-1200

REFERENCES

1. Albin RL, Qin Y, Young AB, Penney JB, Chesselet MF. Preproenkephalin messenger RNA-containing neurons in striatum of patients with symptomatic and presymptomatic Huntington's disease: an in situ hybridization study. *Ann Neurol*. 1991; 30: 542-549.
2. Reiner A, Albin RL, Anderson KD, D'Amato CJ, Penney JB, Young AB. Differential loss of striatal projection neurons in Huntington disease. *Proc Natl Acad Sci U S A*. 1988; 85: 5733-5737.
3. Antonini A, Leenders KL, Spiegel R, et al. Striatal glucose metabolism and dopamine D2 receptor binding in asymptomatic gene carriers and patients with Huntington's disease. *Brain*. 1996; 119(Pt 6): 2085-2095.
4. Richfield EK, O'Brien CF, Eskin T, Shoulson I. Heterogeneous dopamine receptor changes in early and late Huntington's disease. *Neurosci Lett*. 1991; 132: 121-126.
5. van Oostrom J, Dekker M, Willemsen A, de Jong BM, Roos R, Leenders KL. Changes in striatal dopamine D2 receptor binding in pre-clinical Huntington's disease. *Eur J Neurol*. 2009; 16: 226-231.
6. Tabrizi SJ, Ghosh R, Leavitt BR. Huntingtin Lowering Strategies for Disease Modification in Huntington's Disease. *Neuron*. 2019; 101: 801-819.
7. Tabrizi SJ, Leavitt BR, Landwehrmeyer GB, et al. Targeting Huntingtin Expression in Patients with Huntington's Disease. *N Engl J Med*. 2019; 380: 2307-2316.
8. Rodrigues FB, Ferreira JJ, Wild EJ. Huntington's Disease Clinical Trials Corner: June 2019. *J Huntington's disease*. 2019; 8: 363-371.
9. Nopoulos PC, Aylward EH, Ross CA, et al. Coordinators of the Huntington Study G. Smaller intracranial volume in prodromal Huntington's disease: evidence for abnormal neurodevelopment. *Brain*. 2011; 134: 137-142.
10. Siebzehnrubl FA, Raber KA, Urbach YK, et al. Early postnatal behavioral, cellular, and molecular changes in models of Huntington disease are reversible by HDAC inhibition. *Proc Natl Acad Sci U S A*. 2018; 115: E8765-E8774.
11. van der Plas E, Langbehn DR, Conrad AL, et al. Abnormal brain development in child and adolescent carriers of mutant huntingtin. *Neurology*. 2019; 93: e1021-e1030.
12. Molero AE, Arteaga-Bracho EE, Chen CH, et al. Selective expression of mutant huntingtin during development recapitulates characteristic features of Huntington's disease. *Proc Natl Acad Sci U S A*. 2016; 113: 5736-5741.
13. Gray M, Shirasaki DI, Cepeda C, et al. Full-length human mutant huntingtin with a stable polyglutamine repeat can elicit progressive and selective neuropathogenesis in BACHD mice. *J Neurosci*. 2008; 28: 6182-6195.
14. Hult Lundh S, Nilsson N, Soylu R, Kirik D, Petersen A. Hypothalamic expression of mutant huntingtin contributes to the development of depressive-like behavior in the BAC transgenic mouse model of Huntington's disease. *Hum Mol Genet*. 2013; 22: 3485-3497.
15. Hult S, Soylu R, Bjorklund T, et al. Mutant huntingtin causes metabolic imbalance by disruption of hypothalamic neurocircuits. *Cell Metab*. 2011; 13: 428-439.
16. Wang N, Gray M, Lu XH, et al. Neuronal targets for reducing mutant huntingtin expression to ameliorate disease in a mouse model of Huntington's disease. *Nat Med*. 2014; 20: 536-541.
17. Lundh SH, Soylu R, Petersen A. Expression of mutant huntingtin in leptin receptor-expressing neurons does not control the metabolic and psychiatric phenotype of the BACHD mouse. *PLoS One*. 2012; 7: e51168.
18. Soylu-Kucharz R, Baldo B, Petersen A. Metabolic and behavioral effects of mutant huntingtin deletion in Sim1 neurons in the BACHD mouse model of Huntington's disease. *Sci Rep*. 2016; 6: 28322.
19. Baldo B, Cheong RY, Petersen A. Effects of Deletion of Mutant Huntingtin in Steroidogenic Factor 1 Neurons on the Psychiatric and Metabolic Phenotype in the BACHD Mouse Model of Huntington Disease. *PLoS One*. 2014; 9: e107691.
20. Petkau TL, Hill A, Connolly C, et al. Mutant huntingtin expression in microglia is neither required nor sufficient to cause the Huntington's disease-like phenotype in BACHD mice. *Hum Mol Genet*. 2019; 28: 1661-1670.
21. Wood TE, Barry J, Yang Z, Cepeda C, Levine MS, Gray M. Mutant huntingtin reduction in astrocytes slows disease progression in the BACHD conditional Huntington's disease mouse model. *Hum Mol Genet*. 2019; 28: 487-500.
22. Carroll JB, Bates GP, Steffan J, Saft C, Tabrizi SJ. Treating the whole body in Huntington's disease. *Lancet neurology*. 2015; 14: 1135-1142.
23. Child DD, Lee JH, Pascua CJ, Chen YH, Mas Monteys A, Davidson BL. Cardiac mTORC1 Dysregulation Impacts Stress Adaptation and Survival in Huntington's Disease. *Cell Rep*. 2018; 23: 1020-1033.
24. Hoffmann R, Stuwe SH, Goetze O, et al. Progressive hepatic mitochondrial dysfunction in premanifest Huntington's disease. *Mov Disord*. 2014; 29: 831-834.
25. McCourt AC, Parker J, Silajdzic E, et al. Analysis of White Adipose Tissue Gene Expression Reveals CREB1 Pathway Altered in Huntington's Disease. *Journal of Huntingtons Disease*. 2015; 4: 371-382.
26. Patassini S, Begley P, Reid SJ, et al. Identification of elevated urea as a severe, ubiquitous metabolic defect in the brain of patients with Huntington's disease. *Biochem Biophys Res Comm*. 2015; 468: 161-166.
27. Fink JS, Weaver DR, Rivkees SA, et al. Molecular-Cloning of the Rat Adenosine-A2 Receptor - Selective Coexpression with D2-Dopamine Receptors in Rat Striatum. *Mol Brain Res*. 1992; 14: 186-195.
28. Schiffmann SN, Libert F, Vassart G, Vanderhaeghen JJ. Distribution of adenosine A2 receptor mRNA in the human brain. *Neurosci Lett*. 1991; 130: 177-181.

29. Schiffmann SN, Fisone G, Moresco R, Cunha RA, Ferre S. Adenosine A2A receptors and basal ganglia physiology. *Prog Neurogibol*. 2007; 83: 277-292.
30. Baldo B, Sajjad MU, Cheong RY, et al. Quantification of Total and Mutant Huntingtin Protein Levels in Biospecimens Using a Novel alphaLISA Assay. *eNeuro*. 2018; 5.
31. Pouladi MA, Stanek LM, Xie Y, et al. Marked differences in neurochemistry and aggregates despite similar behavioural and neuropathological features of Huntington disease in the full-length BACHD and YAC128 mice. *Hum Mol Genet*. 2012; 21: 2219-2232.
32. Miller S, Hill Della Puppa G, Reidling J, Marcora E, Thompson LM, Treanor J. Comparison of Phosphodiesterase 10A, Dopamine Receptors D1 and D2 and Dopamine Transporter Ligand Binding in the Striatum of the R6/2 and BACHD Mouse Models of Huntington's Disease. *Journal of Huntington's disease*. 2014; 3: 333-341.
33. Gerfen CR, Paletzki R, Heintz N. GENSAT BAC cre-recombinase driver lines to study the functional organization of cerebral cortical and basal ganglia circuits. *Neuron*. 2013; 80: 1368-1383.
34. Burrus CJ, McKinstry SU, Kim N, et al. Striatal Projection Neurons Require Huntingtin for Synaptic Connectivity and Survival. *Cell Rep*. 2020; 30(642–57): e6.
35. Martinez-Mir MI, Probst A, Palacios JM. Adenosine A2 receptors: selective localization in the human basal ganglia and alterations with disease. *Neuroscience*. 1991; 42: 697-706.
36. Kenny PJ, Voren G, Johnson PM. Dopamine D2 receptors and striatopallidal transmission in addiction and obesity. *Curr Opin Neurobiol*. 2013; 23: 535-538.
37. Wang GJ, Volkow ND, Logan J, et al. Brain dopamine and obesity. *Lancet*. 2001; 357: 354-357.
38. Ross CA, Reilmann R, Cardoso F, et al. Movement Disorder Society Task Force Viewpoint: Huntington's Disease Diagnostic Categories. *Mov Disord Clin Pract*. 2019; 6: 541-546.
39. Mantovani S, Gordon R, Li R, Christie DC, Kumar V, Woodruff TM. Motor deficits associated with Huntington's disease occur in the absence of striatal degeneration in BACHD transgenic mice. *Hum Mol Genet*. 2016; 1: 1780-1791.
40. Spampanato J, Gu X, Yang XW, Mody I. Progressive synaptic pathology of motor cortical neurons in a BAC transgenic mouse model of Huntington's disease. *Neuroscience*. 2008; 157: 606-620.
41. Glass M, Dragunow M, Faull RL. The pattern of neurodegeneration in Huntington's disease: a comparative study of cannabinoid, dopamine, adenosine and GABA(A) receptor alterations in the human basal ganglia in Huntington's disease. *Neuroscience*. 2000; 97: 505-519.
42. Popoli P, Blum D, Domenici MR, Burnouf S, Chern YJ. A critical evaluation of adenosine A(2A) receptors as potentially "Druggable" targets in Huntington's disease. *Curr Pharm Des*. 2008; 14: 1500-1511.
43. Tarditi A, Camurri A, Varani K, et al. Early and transient alteration of adenosine A2A receptor signaling in a mouse model of Huntington disease. *Neurobiol Dis*. 2006; 23: 44-53.
44. Mievis S, Blum D, Ledent C. A2A receptor knockout worsens survival and motor behaviour in a transgenic mouse model of Huntington's disease. *Neurobiol Dis*. 2011; 41: 570-576.
45. Estrada-Sanchez AM, Burroughs CL, Cavaliere S, et al. Cortical efferents lacking mutant huntingtin improve striatal neuronal activity and behavior in a conditional mouse model of Huntington's disease. *J Neurosci*. 2015; 35: 4440-4451.
46. Lee JK, Ding Y, Conrad AL, et al. Sex-specific effects of the Huntington gene on normal neurodevelopment. *J Neurosci Res*. 2017; 95: 398-408.
47. Molero AE, Gokhan S, Gonzalez S, Feig JL, Alexandre LC, Mehler MF. Impairment of developmental stem cell-mediated striatal neurogenesis and pluripotency genes in a knock-in model of Huntington's disease. *Proc Natl Acad Sci U S A*. 2009; 106: 21900-21905.
48. Barnat M, Capizzi M, Aparicio E, et al. Huntington's disease alters human neurodevelopment. *Science*. 2020; 369(6505): 787-793.
49. Lendahl U, Zimmerman LB, McKay RD. CNS stem cells express a new class of intermediate filament protein. *Cell*. 1990; 60: 585-595.
50. Dahlstrand J, Lardelli M, Lendahl U. Nestin mRNA expression correlates with the central nervous system progenitor cell state in many, but not all, regions of developing central nervous system. *Brain Res Dev Brain Res*. 1995; 84: 109-129.
51. Sapp E, Kegel KB, Aronin N, et al. Early and progressive accumulation of reactive microglia in the Huntington disease brain. *J Neuropathol Exp Neurol*. 2001; 60: 161-172.
52. Crotti A, Benner C, Kerman BE, et al. Mutant Huntingtin promotes autonomous microglia activation via myeloid lineage-determining factors. *Nat Neurosci*. 2014; 17: 513-521.
53. Khoshnan A, Sabbaugh A, Calamini B, et al. IKKbeta and mutant huntingtin interactions regulate the expression of IL-34: implications for microglial-mediated neurodegeneration in HD. *Hum Mol Genet*. 2017; 26: 4267-4277.
54. Siew JJ, Chen HM, Chen HY, et al. Galectin-3 is required for the microglia-mediated brain inflammation in a model of Huntington's disease. *Nat Commun*. 2019; 10.
55. Ochaba J, Fote G, Kachemov M, et al. IKKbeta slows Huntington's disease progression in R6/1 mice. *Proc Natl Acad Sci U S A*. 2019; 116: 10952-10961.
56. Crapser JD, Ochaba J, Soni N, Reidling JC, Thompson LM, Green KN. Microglial depletion prevents extracellular matrix changes and striatal volume reduction in a model of Huntington's disease. *Brain*. 2020; 143: 266-288.
57. Dubois NC, Hofmann D, Kaloulis K, Bishop JM, Trumpp A. Nestin-Cre transgenic mouse line Nes-Cre1 mediates highly efficient Cre/loxP mediated recombination in the nervous system, kidney, and somite-derived tissues. *Genesis*. 2006; 44: 355-360.
58. Petersen A, Weydt P. The psychopharmacology of Huntington disease. Handbook of clinical neurology / edited by PJ Vinken and GW Bruyn. 2019; 165: 179-189.
59. Friend DM, Devarakonda K, O'Neal TJ, et al. Basal Ganglia Dysfunction Contributes to Physical Inactivity in Obesity. *Cell Metab*. 2017; 25: 312-321.
60. Guo J, Simmons WK, Herscovitch P, Martin A, Hall KD. Striatal dopamine D2-like receptor correlation patterns with human obesity and opportunistic eating behavior. *Mol Psychiatry*. 2014; 19: 1078-1084.
61. Pecina M, Sikora M, Avery ET, et al. Striatal dopamine D2/3 receptor-mediated neurotransmission in major depression: Implications for anhedonia, anxiety and treatment response. *European neuropsychopharmacol: the journal of the European College of Neuropsychopharmacology* 2017; 27: 977-986.
62. Petersen A, Gabery S. Hypothalamic and limbic system changes in Huntington's disease. *J Huntington's Disease*. 2012; 1: 5-16.
63. Cheong RY, Gabery S, Petersen A. The Role of Hypothalamic Pathology for Non-Motor Features of Huntington's Disease. *J Huntington's Disease*. 2019; 8: 375-391.
64. Politis M, Pavese N, Tai YF, Tabrizi SJ, Barker RA, Piccini P. Hypothalamic involvement in Huntington's disease: an in vivo PET study. *Brain*. 2008; 131: 2860-2869.
65. Soneson C, Fontes M, Zhou Y, et al. Early changes in the hypothalamic region in prodromal Huntington disease revealed by MRI analysis. *Neurobiol Dis*. 2010; 40: 531-543.
66. Aziz A, Fronczek R, Maat-Schieman M, et al. Hypocretin and melanin-concentrating hormone in patients with Huntington disease. *Brain Pathol*. 2008; 18: 474-483.
67. Gabery S, Murphy K, Schultz K, et al. Changes in key hypothalamic neuropeptide populations in Huntington disease revealed by neuropathological analyses. *Acta Neuropathol*. 2010; 120: 777-788.
68. Gabery S, Halliday G, Kirik D, Englund E, Petersen A. Selective loss of oxytocin and vasopressin in the hypothalamus in early Huntington disease: a case study. *Neuropathol Appl Neurobiol*. 2015; 41: 843-848.

69. Baldo B, Gabery S, Soylu-Kucharz R, et al. SIRT1 is increased in affected brain regions and hypothalamic metabolic pathways are altered in Huntington disease. *Neuropathol Appl Neurobiol*. 2019; 45: 361-379.
70. Petersen A, Gil J, Maat-Schieman ML, et al. Orexin loss in Huntington's disease. *Hum Mol Genet*. 2005; 14: 39-47.
71. Cheong RY, Tonetto S, von Horsten S, Petersen A. Imbalance of the oxytocin-vasopressin system contributes to the neuropsychiatric phenotype in the BACHD mouse model of Huntington disease. *Psychoneuroendocrinology*. 2020; 119: 104773.
72. Pouladi MA, Morton AJ, Hayden MR. Choosing an animal model for the study of Huntington's disease. *Nat Rev Neurosci*. 2013; 14: 708-721.
73. Wright GEB, Collins JA, Kay C, et al. Length of Uninterrupted CAG, Independent of Polyglutamine Size, Results in Increased Somatic Instability, Hastening Onset of Huntington Disease. *Am J Hum Genet*. 2019; 104: 1116-1126.
74. Genetic Modifiers of Huntington's Disease Consortium. CAG Repeat Not Polyglutamine Length Determines Timing of Huntington's Disease Onset. *Cell*. 2019; 178(887–900): e14.
75. Sobczak K, de Mezer M, Michlewski G, Krol J, Krzyzosiak WJ. RNA structure of trinucleotide repeats associated with human neurological diseases. *Nucleic Acids Res*. 2003; 31: 5469-5482.
76. Mykowska A, Sobczak K, Wojciechowska M, Kozlowski P, Krzyzosiak WJ. CAG repeats mimic CUG repeats in the misregulation of alternative splicing. *Nucleic Acids Res* 2011; 39: 8938-8951
77. Sobczak K, Krzyzosiak WJ. CAG repeats containing CAA interruptions form branched hairpin structures in spinocerebellar ataxia type 2 transcripts. *J Biol Chem*. 2005; 280: 3898-3910.
78. Banez-Coronel M, Ayhan F, Tarabochia AD, et al. RAN Translation in Huntington Disease. *Neuron*. 2015; 88: 667-677.
79. Zeitler B, Froelich S, Marlen K, et al. Allele-selective transcriptional repression of mutant HTT for the treatment of Huntington's disease. *Nat Med*. 2019; 25: 1131-1142.
80. Aronin N, DiFiglia M. Huntingtin-lowering strategies in Huntington's disease: antisense oligonucleotides, small RNAs, and gene editing. *Mov Disord*. 2014; 29: 1455-1461.
81. Monteys AM, Ebanks SA, Keiser MS, Davidson BL. CRISPR/Cas9 Editing of the Mutant Huntingtin Allele In Vitro and In Vivo. *Molecular therapy: the journal of the American Society of Gene Therapy*. 2017; 25: 12-23.
82. Yang S, Chang R, Yang H, et al. CRISPR/Cas9-mediated gene editing ameliorates neurotoxicity in mouse model of Huntington's disease. *J Clin Investig*. 2017; 127: 2719-2724.
83. Boudreau RL, Spengler RM, Davidson BL. Rational design of therapeutic siRNAs: minimizing off-targeting potential to improve the safety of RNAi therapy for Huntington's disease. *Molecular therapy: the journal of the American Society of Gene Therapy*. 2011; 19: 2169-2177.
84. Spronck EA, Brouwers CC, Valles A, et al. AAV5-miHTT Gene Therapy Demonstrates Sustained Huntingtin Lowering and Functional Improvement in Huntington Disease Mouse Models. *Mol Ther Methods Clin Dev*. 2019; 13: 334-343.

SUPPORTING INFORMATION

Additional supporting information may be found online in the Supporting Information section.

Fig S1

Fig S2

Supplementary Material

How to cite this article: Cheong RY, Baldo B, Sajjad MU, Kirik D, Petersén Å. Effects of mutant huntingtin inactivation on Huntington disease-related behaviours in the BACHD mouse model. *Neuropathol Appl Neurobiol*. 2021;47:564–578. https://doi.org/10.1111/nan.12682